Some Applications of Power Spectra to Airplane Turbulence Problems

ROY STEINER* AND KERMIT PRATT†
NASA Langley Research Center, Hampton, Va.

Some of the elements of power spectral density (PSD) methods as applied to the prediction of airplane responses to continuous turbulence are briefly surveyed and are illustrated by some results of both experimental and analytical studies. Included are the descriptions of the turbulence spectra, the airplane frequency-response functions, and the airplane responses. Examples of frequency-response functions determined from calculations, flight tests, and wind-tunnel tests are presented, and the wind-tunnel test technique is described. Also presented is an example of the application of the flight-simulation approach to problems for which PSD methods are not suitable. The results of fatigue tests featuring random loadings having different spectral shapes are reviewed.

I. Introduction

THE treatment of the airplane response to atmospheric turbulence is becoming more closely associated with power spectral density (PSD) techniques. This evolution has occurred over the past 15 years and is probably due generally to two factors. First, the description of atmospheric turbulence as a continuous random function is more realistic and has a more general application in estimating the loads and motions of an airplane in turbulence than the discrete gust method. Second, as airplane designs have evolved, the structures have become progressively more flexible and have been characterized by more readily excitable and poorly damped modes of vibration. The full potential of the power spectral density procedure has not been fully realized, however, and further research is required for its development. Nevertheless, in its present form the technique appears to be the best available for gust load prediction and there are indications that it will be used for airplane design in the near future.

In the application of power spectral density techniques, there are three general fields of interest: the definition of the input or the atmospheric turbulence, the definition of the structural response to a disturbance or the frequency-response function, and the definition of a given output or response. The interpretation of response includes the effect of the response on materials or human beings.

In this paper, these elements of PSD analysis are briefly surveyed and illustrated by some results of both experimental and analytical studies conducted by the NASA, primarily at the Langley Research Center. The survey includes a description of the turbulence in both a random time function and spectrum form. Some frequency-response functions of airplanes based on calculations, flight investigations, and wind-tunnel tests are presented, and the technique used in the wind tunnel is described. Also presented is an example of a problem for which PSD analysis is not suitable. This problem is the effect of turbulence on the deep stall characteristics of a T-tail airplane and was studied by simulating both the flight of the airplane and the turbulence as a random time function. The paper is concluded with a discussion of the results of fatigue tests featuring random loadings having different spectral shapes.

Presented as Paper 66-1000 at the AIAA Third Annual Meeting, Boston, Mass., November 29–December 2, 1966; submitted December 8, 1966; revision received March 9, 1967. [2.09,11.04]

* Aero-Space Technologist, Atmospheric Physics Branch, Dynamic Loads Division.
† Head, Aeroelastic Analysis Section, Aeroelasticity Branch, Dynamic Loads Division.

II. Elements of PSD Analysis

The value of the power spectral density analysis (or generalized harmonic analysis) lies in its ability to relate the statistical descriptions of random airplane responses and atmospheric turbulence by means of a nonstatistical description of the airplane dynamics and without having to analyze the random time function. The theory has been developed for linear systems and for stationary random processes; that is, processes for which the statistical parameters are invariant with time. Individual patches of turbulence fulfill these requirements of stationarity sufficiently so that generalized harmonic techniques may be applied to individual turbulent areas. These turbulent areas extend over 10–30 miles in length for convective activity and up to 50 or more miles for large air mass flows. The theory for the individual patches has then been extended to determine the statistical responses to the over-all flight experience.

Generally, the treatment of the airplane turbulence problem has been based on the concept of a one-dimensional turbulence model. In such a model the effects of spanwise variations in turbulence velocities are assumed to be negligible. A summary of the theoretical considerations in the application of PSD to the turbulence problem may be found in Ref. 1. Listed below are a few fundamental equations relating to this problem.

For the response to individual turbulent areas, the input-output relation is

$$\phi_y(\omega) = \phi_w(\omega)|H(\omega)|^2 \quad (1)$$

where $\phi_y(\omega)$ is the output or response spectrum; $\phi_w(\omega)$ is the input or turbulence spectrum, and $|H(\omega)|$ is the airplane frequency-response function; that is, the response to a one-dimensional, sinusoidal gust field.

The frequency-response function may also be expressed in terms of the cross spectrum ϕ_{wy} in the form

$$H_c(\omega) = \frac{\phi_{wy}(\omega)}{\phi_w(\omega)} \quad (1a)$$

The spectrum can be expressed as the Fourier transform of a statistical quantity, the autocorrelation function $R(\tau)$

$$\phi(\omega) = \frac{2}{\pi}\int_0^\infty R(\tau)\cos(\tau)d\tau \quad (2)$$

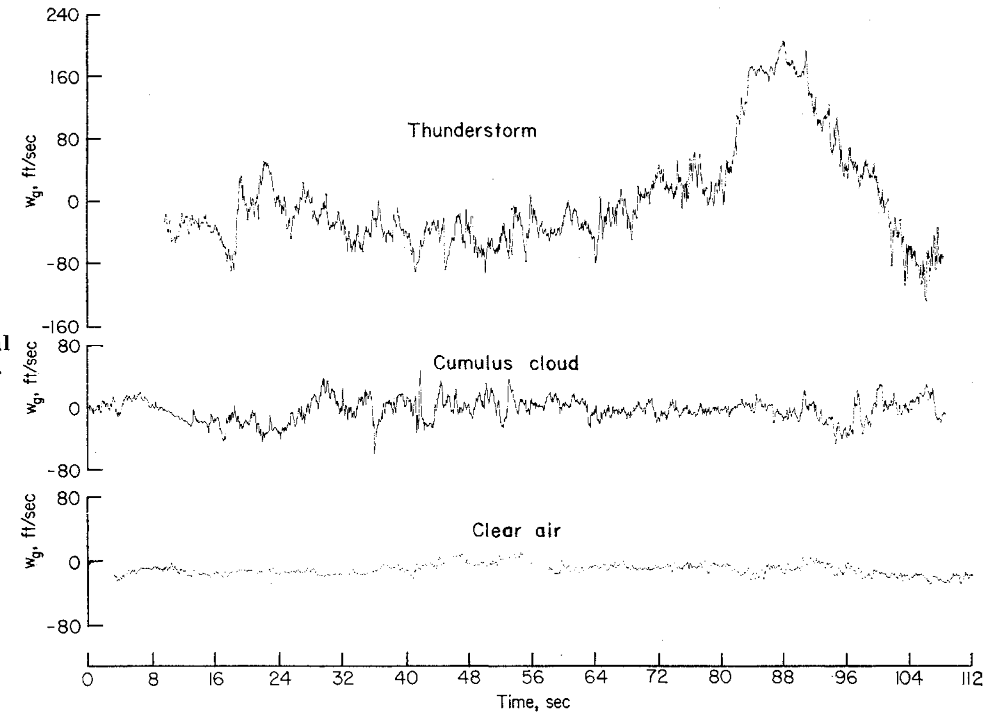

Fig. 1 Time histories of vertical component of true gust velocities.

where

$$R(\tau) = \lim_{T\to\infty} \frac{1}{2T} \int_{-T}^{T} f(t)f(t+\tau)d\tau \tag{3}$$

where in turn $f(t)$ is a random time history, T is a time limit, and τ is the time lag. For short samples the rms value is

$$\sigma = \left[\int_0^\infty \phi(\omega)d\omega\right]^{1/2} \tag{4}$$

and the average number of peaks per unit time that exceed level y is given by

$$N(y) \approx N_0 \exp - (y^2/2\bar{A}^2\sigma_w^2) \tag{5}$$

where

$$N_0 = \frac{1}{2\pi}\left[\frac{\int_0^\infty \omega^2|H(\omega)|^2\phi(\omega)d\omega}{\sigma^2}\right]^{1/2} \tag{6}$$

and where N_0 is the average number of zero crossings with positive slope per unit time of response quantity, y is the response quantity, and $\bar{A}$ is an airplane response parameter equal to σ_y/σ_w. For the over-all turbulence experience (or for continuous variation in σ_w) Eq. (5) takes the form

$$N(y) = N_0 \int_0^\infty p(\sigma_w)\left[\exp - \left(\frac{y^2}{2\bar{A}^2\sigma_w^2}\right)\right]d\sigma \tag{7}$$

where $p(\sigma_w)$ is the probability density function of σ_w. In practice, values of σ_w and $p(\sigma_w)$ are determined from response measurements during routine operations of various airplanes. In the following sections, the components in Eq. (1) are considered in some detail.

Turbulence Spectra

Approximately 15 years ago, the first attempts were made to describe atmospheric turbulence as a continuous random function and to reduce this representation to a spectral form.[2-4] Since the time of these measurements of low-altitude turbulence, additional measurements have been made in cumulus clouds and in severe thunderstorms.[5] In these investigations, from one to three components of the true air velocities were determined from airplane flight tests. Typical time histories of the vertical component of true gust velocities are shown in Fig. 1 for three intensities of turbulence. These intensities are typical for nonstorm or clear-air turbulence, cumulus clouds, and thunderstorms. The time histories were evaluated by use of the relation

$$w_g = V\alpha - V\theta + \int a_z dt + l_x\dot{\theta}$$

where w_g is the vertical component of true turbulence velocities, V is true airspeed, α is the angle of attack from vane, θ is the airplane pitch angle, a_z is the airplane vertical acceleration, l_x is the longitudinal distance from vane to accelerometer, and $\dot{\theta}$ is the airplane pitching velocity. The maximum gust velocities vary from 10 fps for the nonstorm time history to 100 fps or more for the thunderstorm turbulence.

Each of the three time histories in Fig. 1 is random in nature and the more intense turbulence, the top trace, appears to contain a larger proportion of power in the long wavelengths. Power spectral densities calculated from the three time histories by use of Eq. (2) are similar in shape, as shown in Fig. 2. (Longer samples were analyzed in each case than shown in Fig. 1.) The power decreases uniformly with an increase in frequency, and in these cases the power decreases proportionally to a negative $\frac{5}{3}$ power of the frequency. The spectra are displaced uniformly as indicated by the differences in the rms gust velocities.

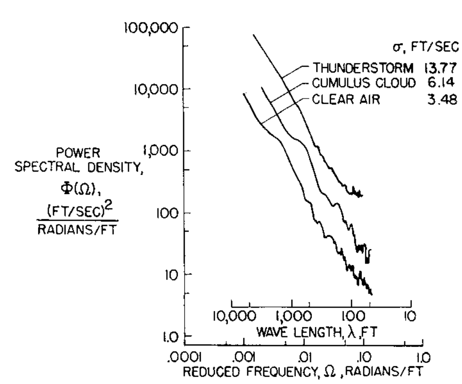

Fig. 2 Representative spectra of atmospheric turbulence for three meteorological conditions.

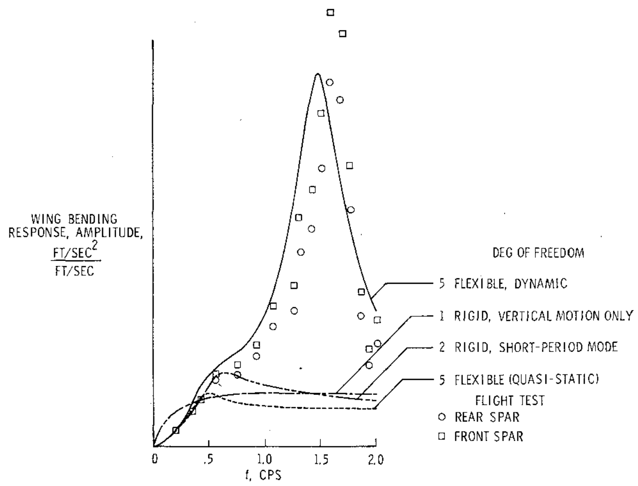

Fig. 3 Calculated and experimental bending-strain frequency responses at 60% semispan for large swept-wing airplane.

The spectra of atmospheric turbulence is normally defined by experimental methods in the wavelength range from 5000 to 10,000 ft as the upper limit down to a wavelength of 50 to 100 ft. The slope and shape of the complete spectrum for wavelengths both above and below these values have been a subject of controversy almost from the time the first spectrum was evaluated. Even in the range defined by experiment, the experimenters report slopes from at least $-\frac{5}{3}$ to -3. Some investigators also report a hump in the spectra (representing the power in standing waves which decay to produce the energy in the shorter wavelengths covered by the spectrum).

It is generally agreed that the power is nearly constant or that the spectra are flat for the very long wavelengths. It is not agreed, however, at what wavelength this change in slope or the knee of the curve exists. These questions are a few of the ones which still remain concerning the description of the input or, in this case, the atmospheric turbulence.

Airplane Frequency Response

The frequency-response function relates the input and the output spectra and is the response due to a sinusoidal gust of varying frequency. It contains the dynamic effects of the various degrees of freedom of the airplane. Three methods have been studied for determining the frequency-response function. These methods are calculations, experimental determination by use of full-scale vehicle, and the experimental determination by use of an aeroelastically scaled model in a specially equipped wind tunnel. The full-scale experimental results may be used to assess the degree of complexity required to represent the dynamics of the airplane for analytical investigations and the adequacy of the design. Both the analytical method and the wind-tunnel or model method may be used in the design of the vehicle. The results of these methods will be reviewed with the major emphasis being given to the flutter model method because of its more recent entrance into the field.

Large flexible airplane

The results of analytical and full-scale flight test investigations of the frequency-response function for wing bending strain at the 60% semispan of a large swept-wing airplane are shown in Fig. 3. The flight test was conducted at a Mach number of 0.58 at an altitude of 5000 ft in clear-air turbulence. The experimental frequency-response functions were obtained by the cross-spectra relation [see Eq. (1a)]. The analytical method and complete results are given in Ref. 6. The calculated frequency-response functions were based on the five degrees of freedom: 1) rigid-body vertical translation, 2) rigid-body pitching, 3) first cantilever wind bending mode, 4) first cantilever wing torsion mode, and 5) the first vertical bending mode of the fuselage as a cantilever beam aft of the center of gravity. The solid curve in Fig. 3 represents the five degrees of freedom or flexible dynamic cases in which the wing bending strain is plotted against frequency in cycles per second. In order to make a comparison between the calculated loads and the measured strains, the strains were normalized by dividing by the strains per g measured in a slow pullup maneuver. Thus, the normalized results have the units of acceleration. The additional curves are based on fewer degrees of freedom or conditions, as indicated in Fig. 3. First to be noted is a considerable loss in accuracy in the region of the short-period frequency (approximately 0.5 cps) when the rigid-body pitch mode is neglected; secondly, the static and dynamic aeroelastic effects of the wing bending mode are considerable as indicated by the large calculated and experimental results which peak at approximately 1.6 cps. These results were some of the first to indicate that an adequate analysis of loads and motions on large flexible airplanes in continuous turbulence could no longer be estimated satisfactorily by using a rigid-body analysis. Some current unpublished data for other airplanes indicate that the accuracy of methods of response calculations involving higher modes of structures needs improving.

Delta-wing fighter

The type of investigation just presented was later applied to a supersonic fighter airplane which featured a delta wing and a pitch damping device. In the flight investigation,[1] flights were made through thunderstorms at a Mach number of 1.3 at 30,000 ft altitude and at a Mach number of 0.92 at an altitude of 35,000 ft. Experimental frequency response was based, in this case, on rigid-body vertical translation and pitching motion only, reflecting the compact and stiff characteristics of the airplane. Some examples of experimental and calculated frequency-response functions for acceleration at the center of gravity and for pitching velocity for both the supersonic and the subsonic speeds are presented in Fig. 4. Calculated results are given for pitch damper both on and off. Both conditions were considered because examination of the flight records indicated that the damper saturated during the flights, that is, elevon deflections in excess of the mechanical limits were commanded by pitch rate but were not realized. The effective damping, therefore, lies somewhere between the values for an inoperative and a fully effective automatic damper. The experimental and calculated functions agree well for the supersonic flight conditions. The agreement is good at the high and low frequencies. The frequency at which the curves peak agrees well and the experimental results lie between the two calculated damping conditions. The functions for the subsonic conditions shown in Fig. 4 do not agree quite as well.

Frequency-response functions from wind-tunnel tests

A more recently developed method of determining the frequency-response function consists of measuring the response of an aeroelastically scaled (flutter) model in simulated free flight through a sinusoidal gust field in a wind tunnel.[7] The apparatus used to generate a nearly one-dimensional gust field in the test section in Langley's Transonic Dynamics Tunnel is shown schematically in Fig. 5. A set of biplane vanes is located on each wall in the converging subsonic portion of the entrance nozzle of the tunnel. The vanes are 3.5 ft in span and have a taper ratio of 0.5 and a panel aspect ratio of 1.2. The two vanes of a biplane set are mechanically inked, and each vane is oscillated about its quarter chord by means of hydraulic motors driving a large flywheel with an offset linkage. Each set of biplanes is driven independently, and control and synchronization are maintained by electronic controls.

The oscillator system was designed for long-duration operation at vane amplitudes from 3° to 12° and at frequencies up to 20 cps. Currently, operation is power-limited as a result of the power absorbed by aerodynamic damping of the vanes. This power limitation gives a frequency limit as a combination of vane angles and dynamic pressure. For 20-cps operation, the dynamic pressure varies from about 60 lb/ft^2 at 12° vane amplitude to about 350 lb/ft^2 at 3° vane amplitude. This latter value is near the maximum dynamic pressure capability of the tunnel in the transonic Mach number range.

Airstream calibrations indicate that the gust velocity is nearly constant in the lateral direction over a distance sufficient for testing a 6-ft-span model. Free flight of the model is simulated by suspending the model in the tunnel test section by cables in such a manner that distortions of the short period and Dutch roll modes are minimized.

Some initial tests were made with a flexible model in order to develop instrumentation, testing, and data reduction techniques; to investigate model flying qualities in such a gust field; and to determine if adequate excitation was available. The model was designed originally for generalized flutter research.

A comparison of the measured center-of-gravity acceleration response with the calculated response is shown in Fig. 6 for a Mach number of 1.0. The results are presented in nondimensional form where the ordinate is the ratio of the normal force coefficient C_n to the stream angle ϵ_g. These values are plotted against the reduced frequency k. Good definition of the response function was obtained near the short-period mode (k of 0.021) and the presence of an oscillatory plunging mode (k of 0.007) due to the cable constraint was indicated.

The agreement between the experimental and calculated results is only fair. Such a result is in part due to the stability derivatives used in the calculations. They were estimated from static force tests of a similar model which differed

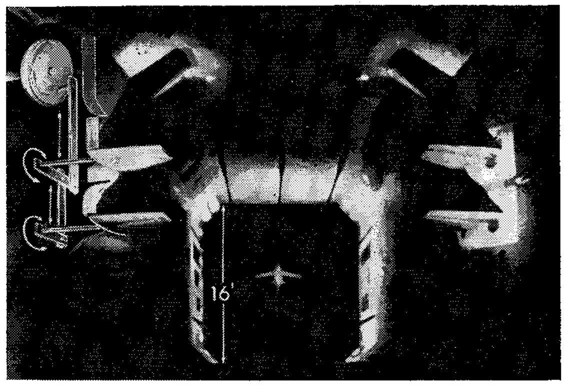

Fig. 5 Vanes and model in the Langley transonic dynamic tunnel showing cutaway of mechanism.

somewhat in flexibility level and fuselage shape from the model tested in the gust field. The model for the force tests also had large engine inlets and internal ducting which were not present in the model used on the dynamic response tests.

From these initial developmental tests of the airstream oscillator, it appears that a means of generating an oscillating airstream of sufficient strength and uniformity has been developed for gust research. Also, a satisfactory means of mounting the model to simulate the free-flight stability modes is available.

III. Application of Spectra to Design

The prediction of airplane motions and loads due to flight in the continuous turbulence of the atmosphere requires that the turbulence spectrum be combined with the airplane frequency responses to obtain response power spectra as indicated by Eq. (1). These spectra, in turn, provide some of the statistical parameters as given by Eqs. (4–7) that are needed to describe the predicted load experience of the airplane.

Efforts to develop this procedure to be a generally acceptable part of airplane design methods have been made for many years and are now being pursued intensively. A recent work is described in Refs. 8 and 9, which present the results of a study by the Lockheed-California Company and the Boeing Company with regard to civil airplanes. A similar study has been made for military airplanes by Dr. J. C. Houbolt of Aeronautical Research Associates of Princeton.[10]

IV. Time Function Studies

As was mentioned earlier, potentially the power spectral method provides statistical parameters for predicting the motions and loads for some airplane designs without requiring an analysis of random time functions of the responses. However, there are some problems which by their nature

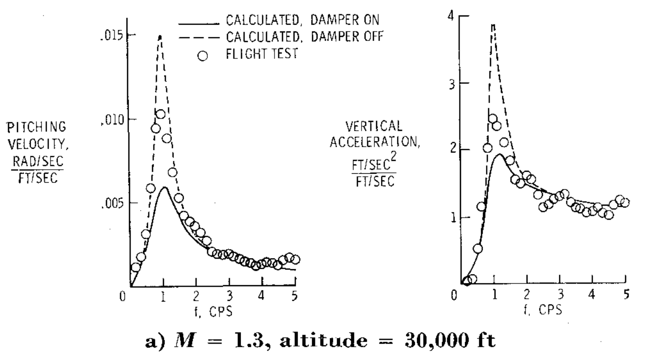

a) M = 1.3, altitude = 30,000 ft

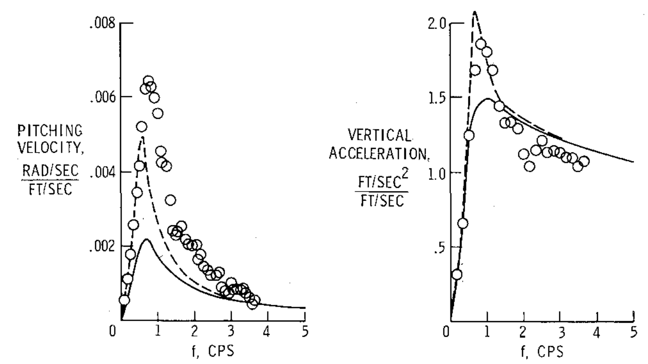

b) M = 0.92, altitude = 35,000 ft

Fig. 4 Frequency responses for delta-wing fighter airplane.

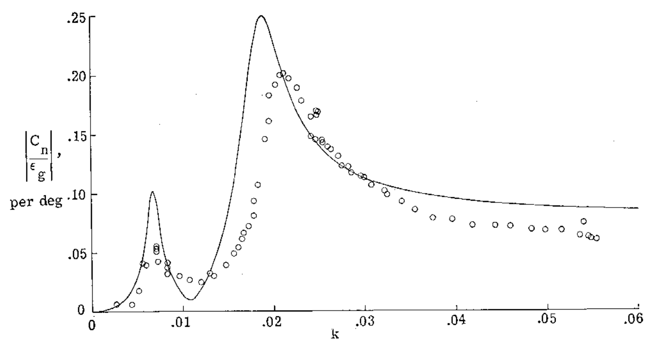

Fig. 6 Comparison of measured and calculated acceleration response for the center of gravity of fighter-type airplane model at M = 1.0.

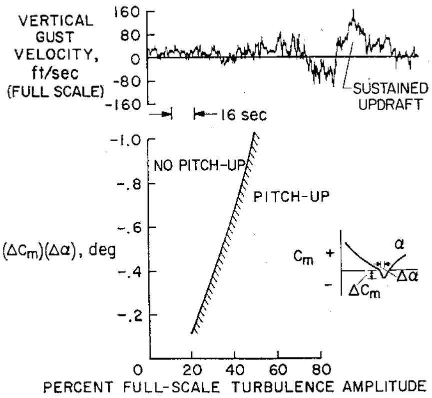

Fig. 7 Boundary for protection against deep stall in turbulence.

cannot be treated by PSD methods, and random time function studies, therefore, must be employed. Such studies also must be made in order to establish the basic functions used in PSD analysis. For example, time function studies were needed to establish the shape of the turbulence spectra and the variations of $N(y)/N_0$ with $y/\bar{A}$ [see Eq. (7)] which reflect the nonstationarity of the random turbulence experienced by airplanes during long periods of service. Two other more recent examples are described in the following section.

Simulation Study

A class of problems for which power spectral analyses are not suitable involves airplane responses which are not linearly related to disturbances. In such cases, the behavior of the airplane is often simulated by an analog computer program which provides motion and load responses from solutions of the nonlinear equations of motion. The effect of flight through atmospheric turbulence is simulated by providing an independent input to the computer through which random time functions representative of gust velocities are introduced. Flight simulators may or may not include human response in the system as, for example, pilot control inputs. Although simulator studies have been made at the Langley Research Center, the study to be described herein is the documented investigation[11] made at the NASA Flight Research Center to determine the effectiveness of a particular technique to reduce the probability of an inadvertent deep stall of a T-tail airplane in flight through turbulence. The simulation computer program included the nonlinear variation of pitching moment coefficient with angle of attack which is characteristic of the T-tail airplane. The effects of a human pilot were not included. The technique of reducing the stall probability consists of providing a sharp increase in the static longitudinal stability $\Delta Cm/\Delta\alpha$ immediately preceding the pitch-up region of angle of attack as indicated in the insert sketch in Fig. 7.

The effects of a number of combinations of values of ΔCm and $\Delta\alpha$ were evaluated from the results of the following test procedure. For each combination of ΔCm and $\Delta\alpha$ the airplane was trimmed at the "knee" of the curve and a series of simulated flights were made through a single random time function of vertical gust velocity. This function was obtained from an actual flight through a thunderstorm. A short sample is shown at the top of Fig. 7. A small fraction of the intensity indicated was used for the initial simulated flight in each series. The intensity (gain) of the gust input was then progressively increased for the subsequent flights until the airplane pitched-up and exceeded the angle of attack corresponding to the minimum value of Cm. It was empirically found that the effects of the variations of ΔCm and $\Delta\alpha$ could be best described by the product $(\Delta Cm) \times (\Delta\alpha)$. The results of the tests are summarized in Fig. 7 by the boundary line between no pitch-up and pitch-up conditions. The boundary is based on the smallest values of $(\Delta Cm)(\Delta\alpha)$ for which pitch-up is avoided while flying in the given gust time function for various percentages of the maximum intensity of the function. The results show that if a pitching moment characteristic represented by larger values of (ΔCm)-$(\Delta\alpha)$ could be devised, then larger intensities of turbulence could be encountered without getting into a pitch-up. It is of interest to note that the critical part of the turbulence time function that triggered pitch-ups most frequently was the sustained updraft indicated in Fig. 7.

V. Fatigue Failure Investigations

Another example of a problem requiring the use of random time functions rather than spectra is the fatigue life of structures under random loads. This, unlike the preceding example, is directly related to power spectral analysis and may be regarded as in the same class of problems as the analysis of random time functions to establish the shape of gust spectra. What is needed is a relation between the fatigue life of the structure and some of the statistical parameters that can be determined from a PSD analysis.

In order to obtain some information on the possibility of such a relation, a number of aluminum alloy specimens were loaded axially by random forces with stationary and Gaussian characteristics and a zero mean value.[12] Three sets of tests were run, each having a different power spectrum of the nominal applied stress. The shapes of the spectra were chosen to be appreciably different and as shown in Fig. 8 were $\phi_1(\omega) = K_1\omega^{-2}$, $\phi_2(\omega) = K_2\omega^0$, $\phi_3(\omega) = K_3\omega^2$ within a pass band of frequencies. These shapes, of course, are not representative of those which are usually experienced by structures in service.

In each of the three sets of tests, a series of specimens was subjected to loads having various rms levels and were tested until rupture occurred. An additional set of tests was made using sinusoidal loadings of various magnitudes to obtain results for comparison with those from the random load tests.

The test specimens were turned from 2024-T4 aluminum alloy with a circular cross section of 0.500-in. diameter and had a theoretical stress concentration factor of 2.2. The loading machine was equipped with a load cell and was driven by a signal from a random noise generator. Suitable filters provided the desired spectral shapes.

During each test, sample time histories of force were recorded and analyzed to verify that the loading function possessed the desired qualities of stationarity and normality of distribution; that the average number of zero crossings and the average number of peaks per sec agreed with theoretical values; and that the rms stress was at the desired level.

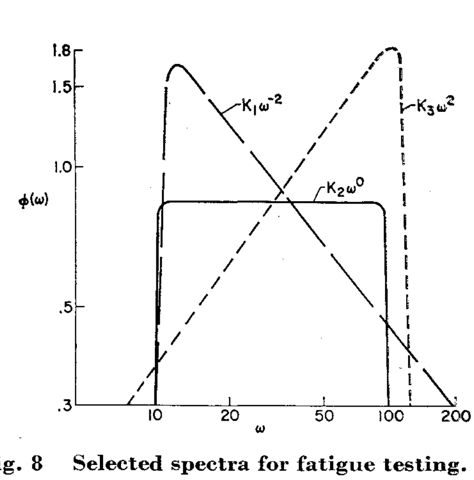

Fig. 8 Selected spectra for fatigue testing.

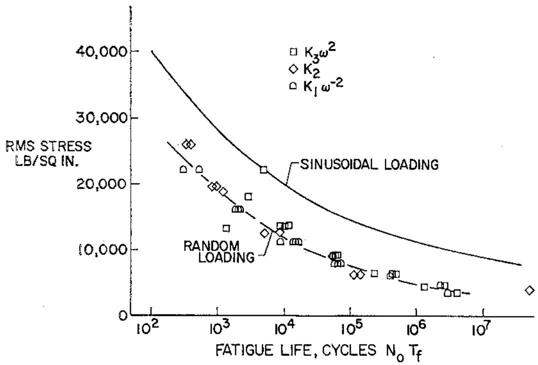

Fig. 9 Random fatigue tests of 2024-T4 aluminum-alloy specimens.

Some of the results of these tests are shown in Fig. 9 wherein the rms applied nominal stress is presented as a function of the fatigue life expressed as the number of effective cycles (the product of the average number of zero crossings with positive slope per sec and the time of rupture). Since the data grouped about the faired dashed curve, it is indicated that neither the large variations in spectral shape nor the smaller variations in the zero crossings (43–67 per sec) had an appreciable effect on the fatigue life. The results from the random loadings would indicate, therefore, that the only significant parameter of those considered is the rms stress value. A comparison of the results of sinusoidal and random loads shows that the fatigue strength for random loads is considerably less than that for sinusoidal loads.

VI. Concluding Remarks

Some of the elements of power spectral density procedures as applied to the prediction of airplane responses to continuous turbulence have been briefly summarized and illustrated by some results of both experimental and analytical studies. Included were descriptions of the turbulence, the frequency-response functions, and the airplane responses. Although the full potential of power spectral density procedures has not been developed, applications of the techniques are gaining wider acceptance.

References

[1] Houbolt, J. C., Steiner, R., and Pratt, K. G., "Dynamic response of airplanes to atmospheric turbulence including flight data on input and response," NASA TR R-199 (1964).

[2] Clementson, G. C., "An investigation of the power spectral density of atmospheric turbulence," PhD Thesis, Massachusetts Institute of Technology (1950).

[3] Notess, C. B. and Eakin, G. J., "Flight test investigation of turbulence spectra at low altitude using a direct method for measuring gust velocities," Cornell Aeronautical Lab. Inc., Rept. VC-839-F-1 (July 1, 1954).

[4] Chilton, R. G., "Some measurements of atmospheric turbulence obtained from flow-direction vanes mounted on an airplane," NACA TN-3313 (1954).

[5] Rhyne, R. H. and Steiner, R., "Power spectral measurements of atmospheric turbulence in severe storms and cumulus clouds," NASA TN D-2469 (1964).

[6] Bennett, F. V. and Pratt, K. G., "Calculated responses of a large sweptwing airplane to continuous turbulence with flight-test comparisons," NASA TR R-69 (1960).

[7] Gilman, J., Jr. and Bennett, R. M., "A wind tunnel technique for measuring frequency-response functions for gust loads analyses," AIAA Paper 65-787 (1965).

[8] Hoblit, F. M., Paul, N., Shelton, J. D., and Ashford, F. E., "Development of a power-spectral gust design procedure for civil aircraft," Lockheed-California Co., FAA-ADS-53 (January 1966).

[9] Fuller, J. R., Richmond, L. D., Larkins, C. D., and Russell, S. W., "Contributions to the development of a power-spectral gust design procedure for civil aircraft," Lockheed-California Co., FAA-ADS-54 (January 1966).

[10] Houbolt, J. C., "Preliminary development of gust design procedures based on power spectral techniques," Volume I: "Theoretical and general considerations," and Volume II: "Summary of possible procedures," Aeronautical Research Associates of Princeton, AFFDL-TR-66-58 (July 1966).

[11] White, M. D. and Cooper, G. E., "Simulator studies of the deep stall," NASA SP-83, pp. 101–111 (1965).

[12] Clevenson, S. A. and Steiner, R., "Fatigue life under various random loading spectra," Shock and Vibration Bull. **35**, 21–31 (January 1966).